

## TEMPERATURE EFFECT ON THE GROWTH RATE AND PHYSICAL CHARACTERISTICS OF SnO<sub>2</sub> THIN FILMS GROWN BY ATOMIC LAYER DEPOSITION

Among the various thin film coating techniques, atomic layer deposition (ALD) has features of good controllability of the thickness, excellent step-coverage in 3-dimensional object even in the sub-nm thickness range at the relatively low deposition temperature. In this study, SnO<sub>2</sub> thin films were grown by ALD in the variation of substrate temperatures from 150 to 250°C. Even such a low temperature may influence on the growth kinetics of the ALD reaction and thus the physical characteristics of thin films, such as crystallinity, film density and optical band gap, etc. We observed the decrease of the growth rate with increasing substrate temperature, at the same time, the density of the film was decreased with increasing temperature. Steric hindrance effect of the precursor molecule was attributed to the inverse relationship of the growth temperature and growth rate as well as the film density. Optical indirect band gap energy (~3.6 eV) of the ALD-grown amorphous SnO<sub>2</sub> films grown at 150°C was similar with that of the literature value, while slightly lower band gap energy (~3.4 eV) was acquired at the films grown at higher temperature.

*Keywords:* atomic layer deposition, tin oxide, growth rate, film density, optical band gap.

### 1. Introduction

SnO<sub>2</sub> is widely used in the various applications, such as gas sensors, transparent electrodes and solar cells [1-3]. Such versatile usages are owing to its useful characteristics, for instance, wide band gap energy (~3.62 eV) and high optical transmittance (~90 %) and good electrical conductivity (0.1–89 Ω cm) [4,5]. Electrical conductivity could be even further increased by adding dopant materials likewise Sb, Nb, Ta, Al, and F [6-9].

SnO<sub>2</sub> film has been prepared with numerous techniques including spray pyrolysis [3,9], atomic layer epitaxy [5], and chemical vapor deposition [10], and atomic layer deposition (ALD) [2,7,8]. Among them, ALD method can precisely control the film thickness and dopant profiles even in 3-dimensional object at the relatively low deposition temperature. Such a good controllability and uniformity enables it to the nanoelectronic applications, for example, display and dynamic random access memory (DRAM) [2,8]. N.H. Lee et al. recently reported that ALD-grown SnO<sub>2</sub> film could be used as a robust friction layer for the triboelectric generator [11]. It was turned out that ALD method was useful in evaluating the dependence of triboelectricity of the friction layer by its thickness and energy band structure of film stack [11].

In this study, SnO<sub>2</sub> films were grown by ALD at the various substrate temperatures. Such a different growth temperature condition affected on the growth rate and physical characteristics of the film. It was revealed that lower growth rate and lower density

of the film was grown at higher growth temperature. Optical band gap energy was also affected by growth temperature. ~3.6 eV of band gap energy was achieved in SnO<sub>2</sub> film grown at 150°C and slightly lower band gap energy (~3.4 eV) was shown in the films grown at higher temperature. It seems that growth kinetics may determine the physical characteristics as well as the growth rate.

### 2. Experimental

The film growth was performed with horizontal traveling-wave-type reactor (CN-1 Co., Atomic Classic, KOREA). TDMA-Sn (Tetrakis(dimethylamino)tin) (UPCHEM Co., KOREA) and water were used as the metalorganic precursor and oxidant, respectively. The substrate temperature was kept at mainly 200°C, while the temperature range of 150 to 250°C was tested. Nitrogen (high purity of 99.9999%) gas was used to control the working pressure with 0.7 mTorr during deposition as well as the purging gas. Process condition is shown in Table 1.

In this study, we investigated the variations of the growth rate and physical properties of SnO<sub>2</sub> films as a function of substrate temperature during the deposition. Optical properties of SnO<sub>2</sub> films were also examined. The film thickness was measured by spectroscopic ellipsometer (MG-1000, NANOVIEW, KOREA) and layer density of the film was characterized by energy-dispersive x-ray fluorescence (EDXRF) (QUANT'X EDXRF Spectrometer, Thermo Fisher Scientific, USA). Optical transmittance

\* SEOUL NATIONAL UNIVERSITY OF SCIENCE AND TECHNOLOGY, SEOUL, KOREA

# Corresponding author: bjchoi@seoultech.ac.kr

and band gap energy of the film was examined by UV-Visible spectrometer (UV-Vis) (Lambda 35, PerkinElmer, USA).

TABLE 1

Deposition process condition

Substrate temperature (°C)	Canister temperature (°C)		Canister gas flow rate (SCCM)	Pressure (mTorr)
	TDMA-Sn	H <sub>2</sub> O	TDMA-Sn	
150-250	30	Room temp.	50	0.7

### 3. Results and discussion

A sequence of ALD reaction is composed of TDMA-Sn feeding – purging – H<sub>2</sub>O feeding – purging pulse. Pulse time of ALD process was determined by examining self-regulation behavior as shown in Figure 1(a-c). First, TDMA-Sn feeding time was set to 1 sec in all the ALD experiment, which was turned out to be sufficient. Next, film growth rate was saturated after 1 sec of H<sub>2</sub>O feeding time. Purging time of TDMA-Sn was determined as 15 sec, while that of H<sub>2</sub>O was not clearly determined due to the absence of saturation behavior. 30 sec of purging time was used in this work. The eventual time sequence of an ALD process was 1-15-1-30 sec. Fig. 1 (d) shows the linear growth of the ALD process and growth rate was determined to 0.48 Å/cycle from the slope of the linear fitted line at 200°C from 100 cycles to 500 cycles.

The density of the film can be calculated by analyzing SnO<sub>2</sub> thin film by using EDXRF. EDXRF can measure the physical quantity of the film as mass per area ( $\mu\text{g}/\text{cm}^2$ ). Dividing by thickness of the film can convert it to mass per volume ( $\text{g}/\text{cm}^3$ ) meaning the density of film. Fig. 2 shows the variation in the area density of the film as a function of the number of ALD cycles at 200°C, while the calculated density of the film was shown in right-axis. Area density of SnO<sub>2</sub> film measured by EDXRF is actually Sn only, so that the density calculated from the area density and thickness only explains the nominal density of Sn. Therefore, the density of the SnO<sub>2</sub> film was estimated from the ratio of anion/cation is kept at 2 and thus atomic weight of Sn and molecular weight of SnO<sub>2</sub> is 118.71 and 148.34 g/mol, respectively. The density of the film was increased to  $\sim 4.5 \text{ g}/\text{cm}^3$  with increasing the number of cycles. However, it was much smaller than the bulk density of the crystalline SnO<sub>2</sub>,  $6.95 \text{ g}/\text{cm}^3$ . The reason of the low density of the film is believed that (1) low crystallinity of as-deposited film, (2) surface roughness and impurities, (3) formation of an interfacial layer on Si substrate.

Growth rate and the physical characteristics of the thin film grown by thermal ALD could be changed by varying its substrate temperature. Figure 3(a) shows differences of area density and thickness depending on the growth temperature. Area density and film thickness were monotonically decreased with increasing growth temperature. 200 cycles of deposition resulted in the film thickness of 16.5 nm at 150°C and 5 nm at 250°C. Generally, this inverse relationship of temperature behavior is

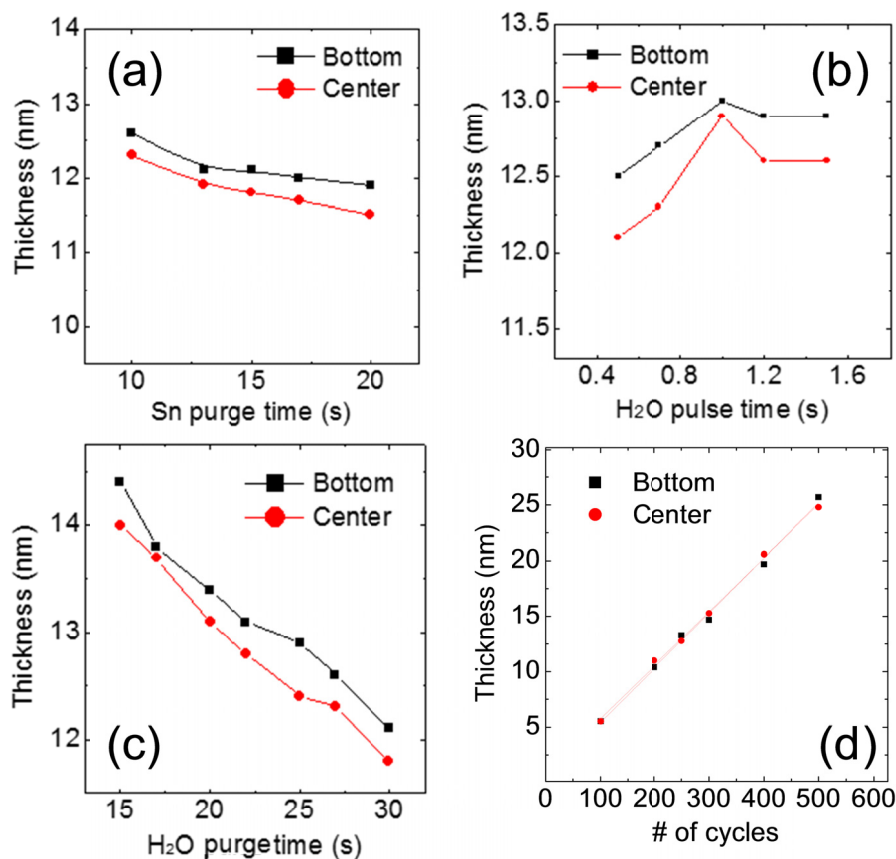


Fig. 1. Saturation growth behavior of SnO<sub>2</sub> film at 200°C of substrate temperature as a function of (a) Sn purge time (b) H<sub>2</sub>O pulse time, and (c) H<sub>2</sub>O purgetime. (d) Thickness of SnO<sub>2</sub> thin film as a function of number of ALD cycles

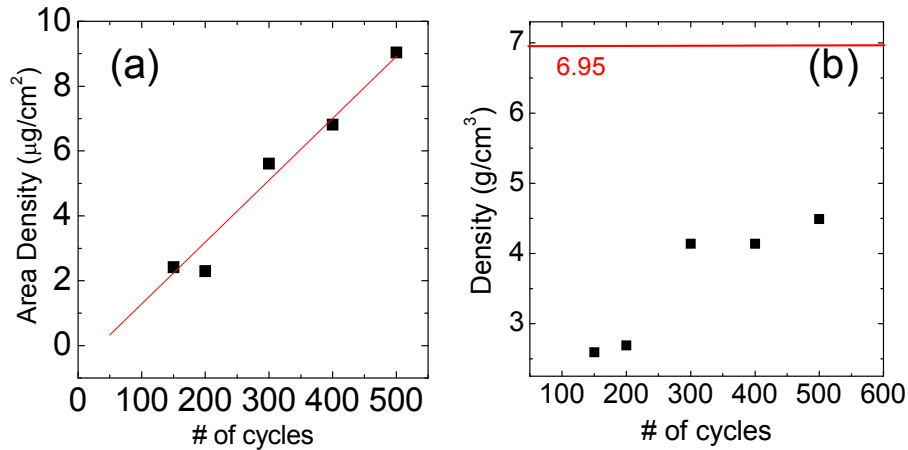


Fig. 2. X-ray fluorescence analysis of SnO<sub>2</sub> thin films, shows (a) area density and (b) density of SnO<sub>2</sub> thin films

known from the steric hindrance effect of ligands in precursor molecule [12]. That is, if there are limited numbers of reaction site on a surface, steric hindrance of the ligands causes saturation of chemisorption, which in turn, the growth rate remains less than a monolayer. Fig. 3 (b) shows the density of the film deposited by 200 cycles at different temperature. The density was less than 4 g/cm<sup>3</sup> in all temperature ranges because the films deposited by 200 cycles are still not thick enough to have a large density as mentioned above. The density of the film is highest at the temperature of 150°C among them. It was considered that steric hindrance effect was less severe at low temperature, so that film surface was more densely packed by its reaction.

The transmittance of SnO<sub>2</sub> film grown on glass substrate was measured by UV-Vis. By subtracting from the transmittance of bare glass substrate as reference sample, transmittance of SnO<sub>2</sub> film itself could be measured. Optical band gap energy can be calculated by absorption coefficient  $\alpha$ . First, absorption coefficient can be calculated from transmittance of the film as following equation;

$$\alpha = \frac{1}{d} \ln\left(\frac{1}{T}\right) \quad (\text{cm}^{-1}) \quad (1)$$

Here,  $d$  is thickness of film (cm) and  $T$  is transmittance of film. Next,  $(\alpha h\nu)^2$  for direct band gap or  $(\alpha h\nu)^{1/2}$  for indirect band

gap can be plotted as a function of energy  $h\nu$  where  $h$  is Planck constant ( $6.626 \times 10^{-34}$  [J·s]) and  $\nu$  can be changed as  $\nu = \lambda/c$  when  $c$  is velocity of light,  $\lambda$  is wavelength of the injected light. The band gap energy can be estimated the intercept of x-axis with the linear-fitted line.

Figure 4 (a) and (b) show the variation in the transmittance and band gap energy by changing growth temperature. The transmittance tends to be lower with decreasing temperature. This means that there is a direct correlation between temperature and thickness. The direct and indirect band gap energy was calculated via a way mentioned above as shown in Fig. 4 (c) and (d). According to Fig. 4 (c) and (d), direct band gap energy and indirect band gap energy of as-grown SnO<sub>2</sub> film grown at 150°C was estimated to  $\sim 4.3$  eV and  $\sim 3.6$  eV, respectively. Indirect band gap energy of bulk SnO<sub>2</sub> is known to be 3.6 eV. Slightly lower band gap energy ( $\sim 4.2$  eV for direct and  $\sim 3.4$  eV for indirect band gap energy) was estimated from the films grown at higher temperature. Such a discrepancy of band gap energy and the noise points from the films with lower density might be originated from the defects at the surface, film itself or interface of the SnO<sub>2</sub> film and glass substrate. Accordingly, band gap energy was also affected by the growth kinetics owing to the growth temperature.

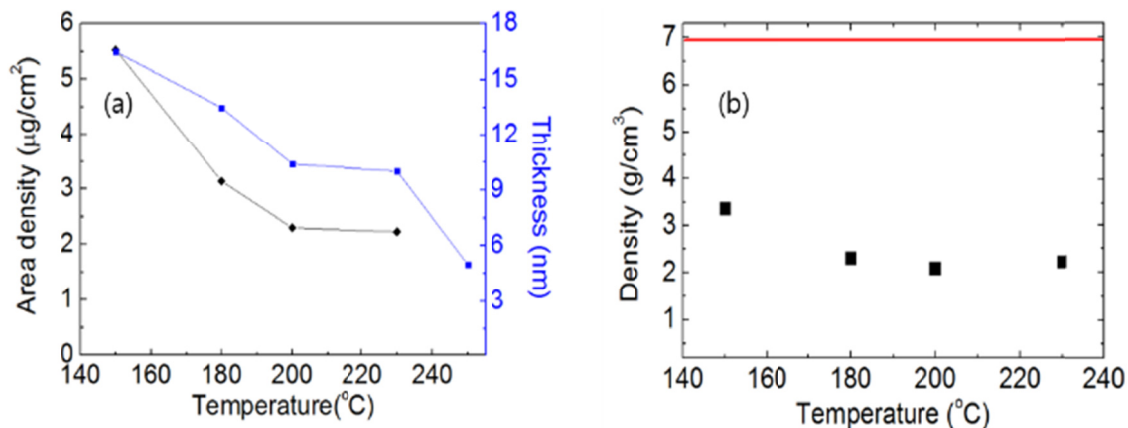


Fig. 3. Variation in the (a) area density and (b) density as a function of deposition temperature

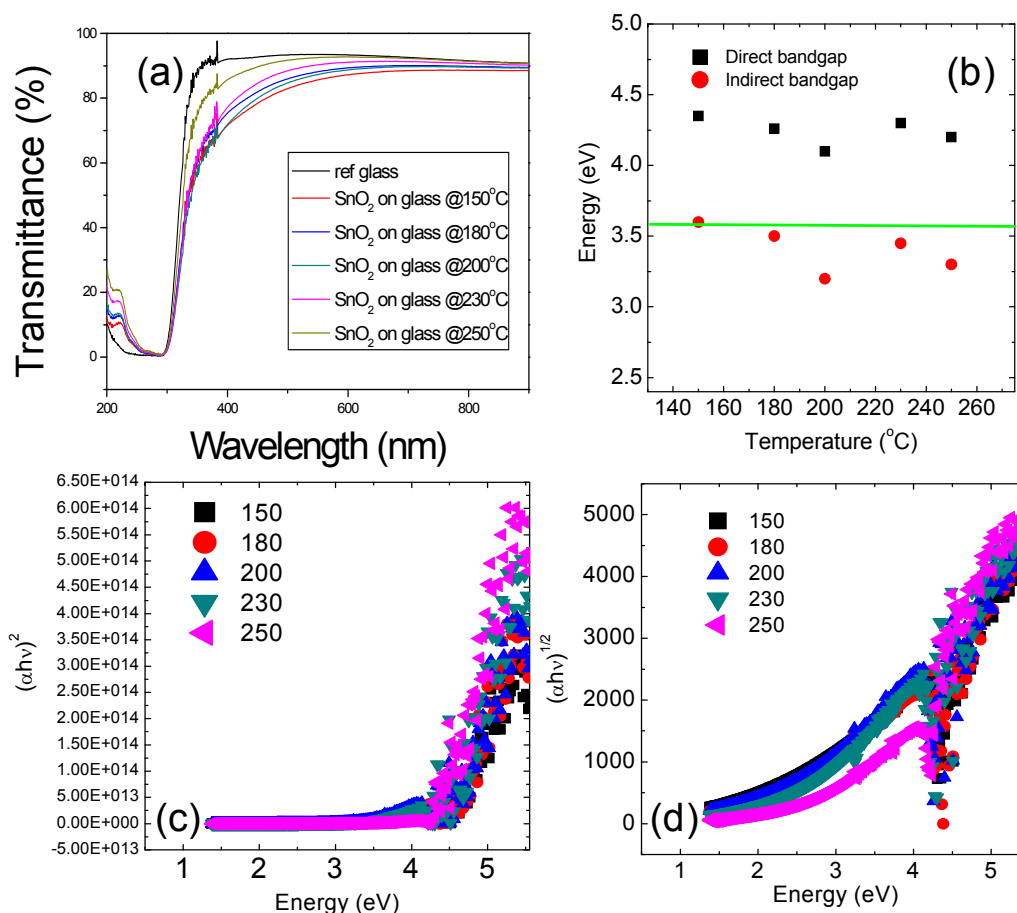


Fig. 4. (a) transmittance of the film (b) direct and indirect band gap energy as a function of temperature. (line is theoretical value, 3.6 eV) Tauc plot of (c) direct and (d) indirect band gap energy

#### 4. Conclusions

SnO<sub>2</sub> thin films were deposited by ALD and their physical characteristics were studied. Growth rate of SnO<sub>2</sub> thin film was 0.48 Å/cycle at 200°C. The density of SnO<sub>2</sub> thin films was estimated by dividing area density by film thickness, which was much lower than the reference value from the literature. We figured out that growth rate was inversely proportional to the growth temperature meaning steric hindrance effect of precursor molecules is dominant. Transmittance and optical bandgap energy could be acquired by UV-Vis, and its indirect bandgap energy was estimated to ~3.6 eV. Therefore, the physical and optical characteristics of the SnO<sub>2</sub> film were dependent on the film growth kinetics. Electrical and chemical characteristics of ALD-grown amorphous SnO<sub>2</sub> thin films should be further examined for its gas sensing application.

#### Acknowledgments

This research was supported by Basic Science Research Program through the National Research Foundation of Korea (NRF) funded by the Ministry of Education (2017R1D1A1A09000809).

#### REFERENCES

- [1] G. Sberveglieri, *Sensors and Actuators B* **6**, 239 (1992).
- [2] D.W. Choi, W.J. Maeng, J.S. Park, *Appl. Surf. Sci.* **313**, 585 (2014).
- [3] S.I. Noh, H.-J. Ahn, D.-H. Riu, *Ceramics International* **38**, 3735 (2012).
- [4] M.M. Abdullah, M.H. Suhail, S.I. Abbas, *Arch. Appl. Sci. Res.* **4**, 1279 (2012).
- [5] M. Utriainen, K. Kovács, J.M. Campbell, L. Niinistö, F. Réti, *J. Electrochem. Soc.* **146**, 189 (1999).
- [6] Y. Wang, T. Brezesinski, M. Antonietti, B. Smarsly, *ACS Nano* **3**, 1373 (2009).
- [7] J. Heo, Y. Liu, P. Sinsersuksakul, Z. Li, L. Sun, W. Noh, R.G. Gordon, *J. Phys. Chem. C* **115**, 10277 (2011).
- [8] C.J. Cho, M.-S. Noh, W.C. Lee, C.H. An, C.-Y. Kang, C.S. Hwang, S.K. Kim, *J. Mater. Chem. C* **5**, 9405 (2017).
- [9] C.-Y. Kim, D.-H. Riu, *Thin Solid Films* **519**, 3081 (2011).
- [10] J.L. Vossen, E.S. Poliniak, *Thin Solid Films*, **13**, 281 (1972).
- [11] N.H. Lee, S.Y. Yoon, D.H. Kim, S.K. Kim, B.J. Choi, *Electronic Materials Lett.* **13**, 318 (2017).
- [12] R.L. Puurunen, *Chemical Vapor Deposition* **9**, 249 (2003).